

# Macroscopically Aligned Helical Conjugated Polymers in Orientation-Controllable Chiral Nematic Liquid Crystal Field

Taizo Mori,<sup>†</sup> Tetsuya Sato,<sup>‡</sup> Mutsumasa Kyotani,<sup>§</sup> and Kazuo Akagi<sup>\*,†</sup>

Department of Polymer Chemistry, Kyoto University, Kyoto 615-8510, Japan, and Tsukuba Research Center for Interdisciplinary Materials Science (TIMS) and Institute of Materials Science, University of Tsukuba, Ibaraki 305-8577, Japan

Received January 3, 2009; Revised Manuscript Received February 4, 2009

**ABSTRACT:** Horizontally and vertically aligned helical polyacetylenes (H-PAs) are synthesized by using orientation-controlled chiral nematic liquid crystals (N\*-LCs) consisting of vertical orientation inducers, chiral dopants and parent N-LC. The chemically graspable pictures of horizontal and vertical N\*-LCs and the corresponding macroscopically aligned H-PAs are put forward as a guideline of the syntheses of the N\*-LCs and H-PAs. It is found that the present N\*-LCs show horizontal and vertical orientations, although they include the vertical orientation inducer. Systematic examinations indicate that the horizontal or vertical orientation of the N\*-LC sensitively depends on (i) the relative concentrations of the vertical orientation inducer and the chiral dopant, (ii) the miscibility of the vertical orientation inducer to the parent N-LC, and (iii) the helical twisting power of the chiral dopant. In other words, the balance in effective strength between the vertical orientation inducer and the chiral dopant dominates the macroscopic orientation of the N\*-LC and hence the morphological alignment of the H-PA.

## 1. Introduction

Macroscopically controlled alignment in conjugated polymers is desirable to enable the exploitation of various inherent properties by way of polymer assembling-assisted intensification or amplification of the properties.<sup>1,2</sup> Since the first use of a chiral nematic liquid crystal (N\*-LC) in asymmetric synthesis to give helical polyacetylene (H-PA),<sup>3</sup> polymerization using N\*-LC as a solvent has become a promising way to synthesize helical conjugated polymers starting from achiral monomers.<sup>4</sup> The N\*-LC is prepared through the addition of a small amount of chiral compound, as a chiral dopant, into a nematic LC (N-LC).<sup>5</sup> This allows us to control the helical power and helical sense of the N\*-LC by tuning the helical twisting power (HTP) and chirality of the chiral dopant.<sup>6</sup>

Meanwhile, the helical fibrils of the H-PAs synthesized hitherto are horizontally aligned because the N\*-LC used for acetylene polymerization has a horizontal alignment (see Figure 1-d).<sup>3</sup> However, the vertically aligned fibril morphologies of H-PA are not comprehensively exploited up to now. It is therefore desired to develop the vertical N\*-LC useful for the synthesis of vertically aligned H-PA.

Previously, we found that the vertically aligned PA is synthesized in the N-LC including a *vertical orientation inducer* which has two phenylcyclohexyl (PCH) mesogenic moieties linked with a flexible methylene chain.<sup>7</sup> The preliminary study indicated that the vertically aligned H-PA can also be synthesized in the vertical N\*-LC, when it is prepared by adding both the chiral dopant and the vertical orientation inducer into the parent N-LC.<sup>7</sup> However, through the above preliminary study, we encountered several subjects to be solved for the construction of the orientation-controlled asymmetric reaction field; (i) No chemically graspable description of the vertical N\*-LC is given, as a guideline, making it difficult to disclose the synthetic conditions for the vertically aligned H-PA. (ii) The helical twisting power of the axially chiral *di*-substituted binaphthyl

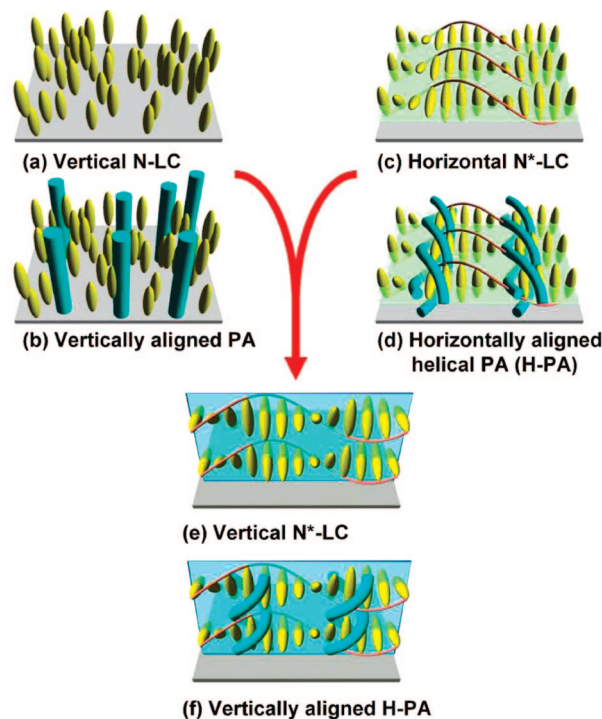


**Figure 1.** Schematic representations of vertical N-LC (a), vertically aligned PA (b), horizontal N\*-LC (c), horizontally aligned helical PA [H-PA] (d), vertical N\*-LC (e), and vertically aligned H-PA (f).

derivative, used as a chiral dopant, is not strong enough for giving sufficiently screwed fibrils of H-PA in the existence of the vertical orientation inducer. (iii) The formation of the vertical N\*-LC is less reproducible, because it sensitively depends on the relative concentration of the vertical orientation inducer and the chiral dopant in the N\*-LC.

Here, we have carried out systematic studies of the N\*-LCs and the resultant H-PAs, by presenting mechanistic pictures of horizontal and vertical N\*-LCs and the horizontally and vertically aligned H-PAs, by using newly synthesized *tetra*-substituted binaphthyl derivatives with large helical twisting

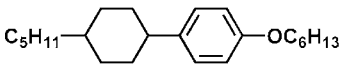
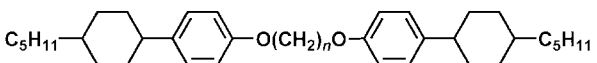
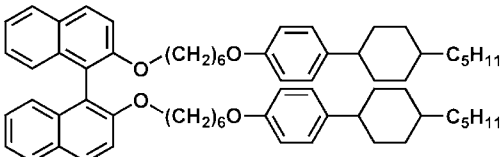
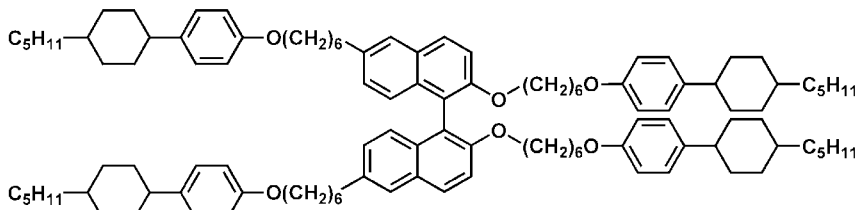
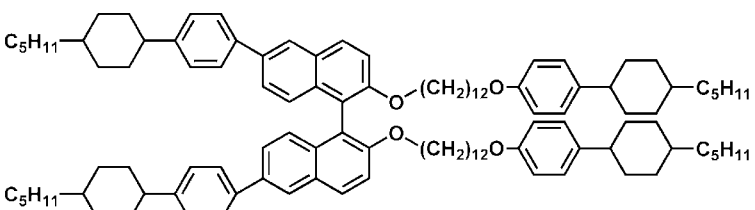
\* Corresponding author. E-mail: akagi@star.polym.kyoto-u.ac.jp.

<sup>†</sup> Department of Polymer Chemistry, Kyoto University.

<sup>‡</sup> Institute of Materials Science, University of Tsukuba.

<sup>§</sup> Tsukuba Research Center for Interdisciplinary Materials Science (TIMS), University of Tsukuba.

Table 1. Molecular Structures of Parent Liquid Crystal, Vertical Orientation Inducers, and Chiral Dopants

Parent liquid crystal	 <p>PCH506</p>
Vertical orientation inducers	 <p>(PCH50)<sub>2n</sub>, (<i>n</i> = 6, 8)</p>
Chiral dopants	 <p>(<i>R</i>)- or (<i>S</i>)-D1</p>
	 <p>(<i>R</i>)- or (<i>S</i>)-D2</p>
	 <p>(<i>R</i>)- or (<i>S</i>)-D3</p>

powers, and also by changing the relative concentrations of the vertical orientation inducer and the chiral dopants in N\*-LCs.

## 2. Chiral Nematic Liquid Crystal Fields and Resultant Products

The comprehensive description of the N\*-LC fields and the polymerization products are shown in Figure 1. Figure 1-a and 1-b show the vertical (homeotropic) N-LC and the vertically aligned PA, respectively. The vertical N-LC can be prepared by adding the vertical orientation inducer into the horizontal (homogeneous) N-LC used as a parent N-LC. Figure 1-c and 1-d show the horizontal N\*-LC and the helical PA (H-PA), respectively. The horizontal N\*-LC can be prepared by adding the chiral dopant into the horizontal N-LC. The H-PA is lying on the substrate, namely the helical axis of the H-PA is parallel to the surface of the substrate. It should be emphasized that the H-PA grows along the direction orthogonal to the helical axis of the N\*-LC, and that the helical sense of the H-PA and that of the N\*-LC are opposite to each other. These facts have been

currently disclosed and will be discussed in details elsewhere.<sup>3g,i</sup>

Figure 1-e and 1-f show the vertical N\*-LC and the vertically aligned H-PA, respectively. The vertical N\*-LC can be prepared by adding both the chiral dopant and the vertical orientation inducer into the parent N-LC under appropriate mole ratios for them. The helical axis of the vertical aligned H-PA is also orthogonal to that of the vertical N\*-LC. It is of importance that the "orthogonal" relationship in the helical axis between the H-PA and N\*-LC holds, irrespective of the alignment of the N\*-LCs.

## 3. Experimental Section

**3.1. Preparation of Liquid Crystals as Reaction Fields.** Table 1 shows molecular structure of the N-LC, the vertical orientation inducers and the chiral dopants. The parent N-LC, PCH506, was synthesized according to the previous work.<sup>7</sup> The vertical orientation inducers with hexa- and octa-methylene chains, (PCH50)<sub>2</sub>6 and (PCH50)<sub>2</sub>8, were synthesized using the methods similar to that for

**Table 2. Concentrations and Helical Pitches of N\*-LCs**

chiral dopant	system	mole ratios between components of N*-LCs	helical pitch ( $\mu\text{m}$ )
D1	1	PCH506:(PCH50) <sub>2</sub> 6:(R)-D1 = 100:3:2	3.6
	2-1	PCH506:(PCH50) <sub>2</sub> 8:(R)-D1 = 100:3:1	5.8
	2-2	PCH506:(PCH50) <sub>2</sub> 8:(R)-D1 = 100:3:2	3.1
D2	3-1	PCH506:(PCH50) <sub>2</sub> 6:(R)-D2 = 100:5:0.5	2.3
	3-2	PCH506:(PCH50) <sub>2</sub> 6:(R)-D2 = 100:5:1	1.2
	4	PCH506:(PCH50) <sub>2</sub> 6:(R)-D2 = 100:10:1	1.1
	5-1	PCH506:(PCH50) <sub>2</sub> 8:(R)-D2 = 100:3:0.5	2.4
	5-2	PCH506:(PCH50) <sub>2</sub> 8:(R)-D2 = 100:3:1	1.2
	6-1	PCH506:(PCH50) <sub>2</sub> 8:(R)-D2 = 100:5:0.5	2.3
	6-2	PCH506:(PCH50) <sub>2</sub> 8:(R)-D2 = 100:5:1	1.1
	7-1	PCH506:(PCH50) <sub>2</sub> 8:(R)-D2 = 100:10:0.5	2.4
	7-2	PCH506:(PCH50) <sub>2</sub> 8:(R)-D2 = 100:10:1	1.1
	D3	8	PCH506:(PCH50) <sub>2</sub> 6:(R)-D3 = 100:10:0.5

PCH506. Axially chiral binaphthyl derivatives, bearing LC substituents at the 2,2'-positions of the binaphthyl rings, (R)- or (S)-2,2'-PCH506-1,1'-binaphthyl [abbreviated as (R)- or (S)-D1],<sup>3</sup> and LC substituents at the 2, 2' and 6, 6' positions of the binaphthyl ones, (R)- or (S)-2,2'-6,6'-PCH506-1,1'-binaphthyl [abbreviated as (R)- or (S)-D2], and (R)- or (S)-2,2'-PCH5012-6,6'-PCH5-1,1'-binaphthyl [abbreviated as (R)- or (S)-D3], were synthesized along the previously reported procedure.<sup>6b,8</sup>

Table 2 summarizes the concentration ratios and the helical pitches of the N\*-LCs. The N\*-LCs of systems 1 and 2 were respectively prepared by adding 3 mol % of the vertical orientation inducers, (PCH50)<sub>2</sub>6 and (PCH50)<sub>2</sub>8, as well as 1–2 mol % of the chiral dopant, D1, into the parent LC, PCH506. The N\*-LCs of systems 3 to 7 were prepared by adding 3–10 mol % of (PCH50)<sub>2</sub>6 or (PCH50)<sub>2</sub>8, as well as 0.5–1 mol % of D2 into PCH506. The N\*-LC of System 8 was prepared by adding 10 mol % of (PCH50)<sub>2</sub>6 and 0.5 mol % of D3 into PCH506.

Polarizing optical microscope (POM) observations of the N\*-LCs were carried out under crossed Nicols by using a NIKON ECLIPSE E400 POL polarizing optical microscope, equipped with a NIKON COOLPIX 950 digital camera, a Linkam TH-600PM, and L-600 heating and cooling stage with temperature control. All N\*-LC showed a fingerprint texture characteristic of helical structure in POM. The phase transition temperatures of the chiral dopants and the N\*-LC were determined using a Perkin-Elmer differential scanning calorimeter (DSC 7) and a TA Instrument Q100 DSC apparatus at a constant heating and cooling rate of 10 °C/min, where the results in the first cooling and the second heating processes were recorded.

The helical pitches of N\*-LCs were evaluated with Cano's wedge method, which was based on the observation of discontinuity lines that appeared when an N\*-LC was inserted into a cell with a gradient thickness.<sup>9</sup> Meanwhile, when the helical pitch was smaller than 1  $\mu\text{m}$ , it was evaluated with the selective light reflection method.<sup>10</sup> The helical pitch was evaluated according to the equation,  $p = \lambda_{\text{max}}/n$ , where  $\lambda_{\text{max}}$  is the center wavelength for the maximally reflected light, and  $n$  is the mean refraction index of N\*-LC ( $n = 1.5$ ). The absolute value of HTP ( $\beta_M$ ), defined as  $\beta_M = (pc)^{-1}$ , was evaluated as the reciprocal of the product between the helical pitch ( $p$ ) and the mole fraction of the chiral dopant ( $c$ ).<sup>11</sup>

**3.2. Acetylene Polymerization.** The N\*-LCs thus prepared were used as an acetylene polymerization solvent for Ziegler–Natta catalyst consisting of Ti(O-*n*-Bu)<sub>4</sub> and Et<sub>3</sub>Al. Typical concentration of Ti(O-*n*-Bu)<sub>4</sub> was 50 mmol/L, and the mole ratio of [Al]/[Ti] was 4. The catalyst solution was aged for 30 min at room temperature. During aging, the N\*-LCs containing the catalyst showed no noticeable change in their optical texture and only a slight lowering of the transition temperature by 1–3 °C.

The catalyst solution was added into a flat-bottom container placed in a Schlenk flask, by using a syringe that was warmed beforehand in order to remain a fluidity of the highly viscous catalyst solution. The Schlenk flask was connected to a vacuum line via a flexible joint and then degassed. The acetylene polymerization was carried out by introducing acetylene gas into the catalyst-containing N\*-LC. Polymerization temperature was kept

constant at 39 °C to maintain the N\* phase, by circulating water through an outer flask enveloping the Schlenk flask. Acetylene gas of six-nine grades was used without further purification. Polymerization temperature was controlled by immersing the whole part of the Schlenk flask in temperature-controlled water bath. The initial acetylene pressure was about 40 Torr and polymerization time was 5 min. After polymerization, PA film was washed with purified toluene several times and with a 1 N HCl–methanol mixture and with THF under argon at room temperature. The film was dried through vacuum pumping on Teflon sheet and stored in a freezer at –20 °C. The thickness of the films was in the range 3–6  $\mu\text{m}$ .

Ultramicrotome apparatus was used to observe the cross section of the PA film. The PA was placed with two sheets of Teflon and put in the plastics container of the capsule type. The film was embedded in an epoxide resin, Eopk 812 (Oken Trading). The epoxide resin was polymerized at 60 °C for about 24 h. The PA film was cut with an ultramicrotome. The cross section of the PA film was observed by transmission electron microscope (TEM).

## 4. Results and Discussion

**4.1. Characterization of N\*-LCs.** The screw directions of the N\*-LCs were determined through the miscibility test (contact method).<sup>12</sup> The miscibility test is based on the observation of the mixing area between the N\*-LC and the standard LC in POM. Cholesteryl oleyl carbonate is known to be a left-handed N\*-LC (cholesteric LC), and therefore it is useful for the standard LC for the miscibility test. If the screw direction of the N\*-LC is the same as that of the standard LC, the mixing area will be continuous. Otherwise, it will be discontinuous (shown as a Schlieren texture of the N-LC). The miscibility test indicated that the N\*-LCs induced by (R)-chiral dopants (D1–D3) have right-handed screw structures and those by (S)-chiral dopants have left-handed ones.

Table 3 summarizes the phase transition temperatures of the N\*-LCs. Systems 1–7 showed N\* and smectic (S) phases in cooling process, but only the N\* phase in the heating process. System 8 showed N\* and S phases in both cooling and heating process. The temperature region of the N\* phase becomes narrow as the concentration of the chiral dopant increases. For instance, system 2-1 [PCH506:(PCH50)<sub>2</sub>8:(R)-D1 = 100:3:1] showed the N\* phase in the region of 37–47 °C in the heating process. However, system 2-2 [PCH506:(PCH50)<sub>2</sub>8:(R)-D1 = 100:3:2] showed the N\* phase in the region of 35–42 °C in the heating process. This is because the miscibility of the chiral dopant itself to the parent N-LC decreases.

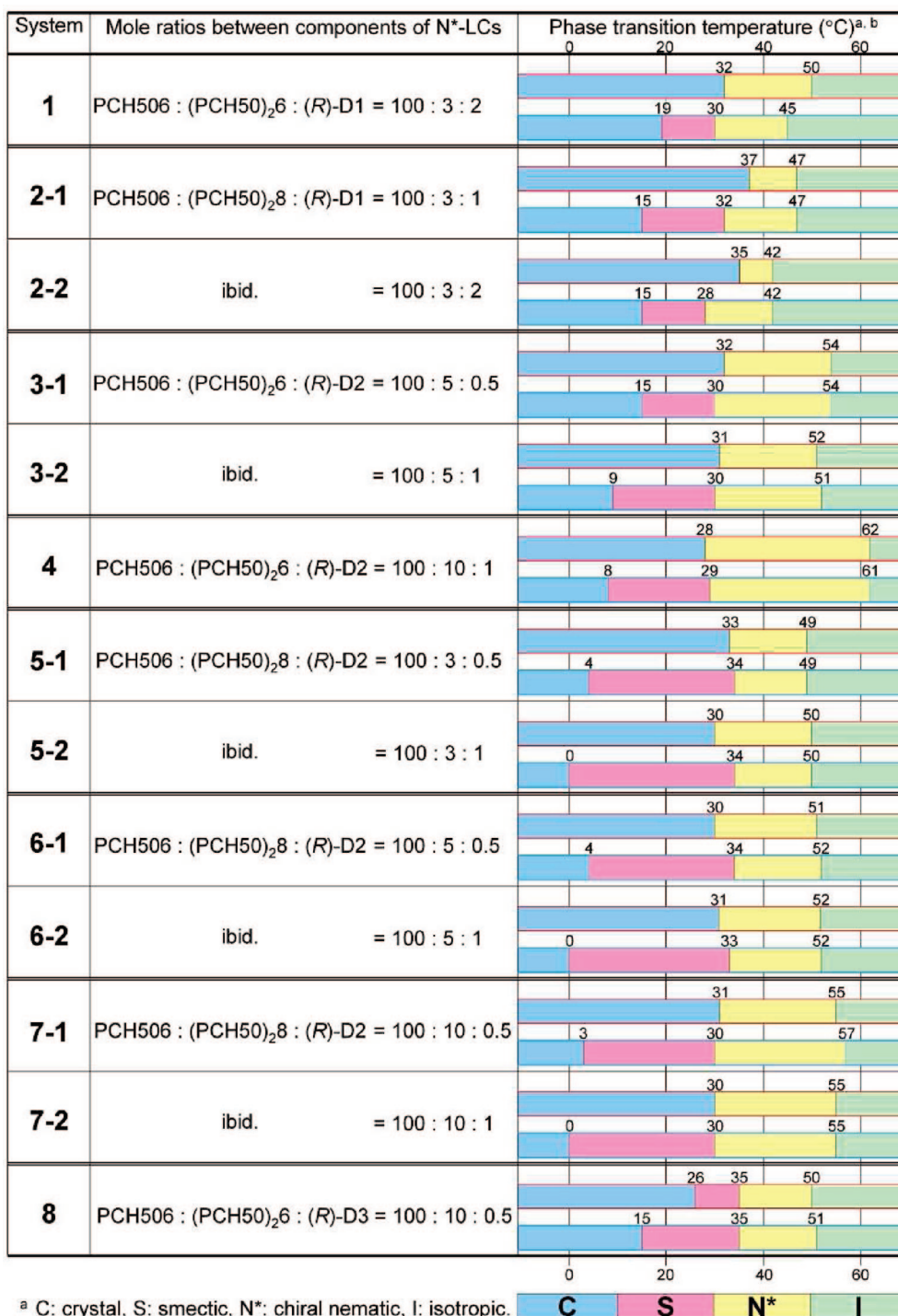
Table 4 summarizes the helical pitches of the N\*-LCs. The helical pitches of Systems 1 to 7 (including D1 ~D2) were evaluated with Cano's wedge method. This method was based on the observation of the distance between discontinuity lines that appeared when the N\*-LC was inserted into a cell with a gradient thickness. The helical pitches of N\*-LCs varied from 5.6 to 3.0  $\mu\text{m}$  with a change of the mole percentage of D1 (from 1.0 to 2.0 mol %), and from 2.4 to 1.1  $\mu\text{m}$  with D2 (from 0.5 to 1.0 mol %).

On the other hand, the helical pitch of system 8 (including D3) was evaluated with the selective light reflection method, because the helical pitch of system 8 is too short to be observed in the Cano's wedge method. The center wavelength for the maximally reflected light ( $\lambda_{\text{max}}$ ) was 1380 nm. Thus, the helical pitch of system 8 was evaluated to be 920 nm by using the equation  $p = \lambda_{\text{max}}/n$  ( $n = 1.5$ ).

The HTPs ( $\beta_M$ ) of D1 and D2 were 18 and 90  $\mu\text{m}^{-1}$ , respectively. It is clear that the HTP of the chiral dopant D2 is 5 times larger than that of D1. This may be rationalized with a difference in the number of substituents. Namely, the axially twisting torque of D2 is more effectively transferred to environmental N-LC molecules, by virtue of intermolecular



Table 3. Phase Transition Temperatures of N\*-LCs



interactions between four PCH substituents of D2 and the PCH moieties of LC molecules, rather than in the case of D1 bearing two PCH substituents.

Besides, the HTP of D3 was evaluated to be  $240 \mu\text{m}^{-1}$ , which is ca. 2.7 times larger than that ( $90 \mu\text{m}^{-1}$ ) of D2. The structural difference between D2 and D3 is that the PCH moieties are indirectly and directly linked with the 6,6' positions of the binaphthyl rings, respectively. That is, the absence of the hexamethylene spacer,  $[-(\text{CH}_2)_6-]$  leads to a rigidity in the linkage between the PCH moieties and the binaphthyl rings of D3, resulting in a larger HTP of D3 than that of D2.

**4.2. Liquid Crystallinity of the Chiral Dopant.** Here it is important to emphasize the liquid crystallinity of the chiral dopant itself. As shown in Table 4, the helical pitches of the N\*-LCs induced by D2 and D3 (systems 3 to 8) were shorter than those by D1. This is partly because D2 and D3 have larger HTPs than D1, and partly because they have a higher miscibility to the parent N-LC than D1. The latter is due to the fact that D2 and D3 have liquid crystallinity.<sup>6b,8</sup> The high miscibility of the chiral dopant allows to increase the concentration of the chiral dopant for preparation of highly twisted N\*-LC and also to enlarge the temperature region of the N\* phase. The wide

**Table 4. Helical Pitches of N\*-LCs and Structural Parameters of H-PAs**

system	N*-LC		H-PA			
	mole ratios between components of N*-LCs	Helical pitch ( $\mu\text{m}$ )	Interdistance between fibril bundles ( $\mu\text{m}$ )	Diameter of a fibril bundle ( $\mu\text{m}$ )	Diameter of a fibril (nm)	direction of fibrils
1	PCH506:(PCH50) <sub>2</sub> 6:(R)-D1 = 100:3:2	3.6	1.7 ( $\pm 0.2$ )	0.9 ( $\pm 0.2$ )	~200	vertically
2-1	PCH506:(PCH50) <sub>2</sub> 8:(R)-D1 = 100:3:1	5.8	2.8 ( $\pm 0.2$ )	0.6 ( $\pm 0.2$ )	~200	vertically
2-2	PCH506:(PCH50) <sub>2</sub> 8:(R)-D1 = 100:3:2	3.1	1.5 ( $\pm 0.2$ )	0.6 ( $\pm 0.2$ )	~200	vertically and horizontally
3-1	PCH506:(PCH50) <sub>2</sub> 6:(R)-D2 = 100:5:0.5	2.3	1.2 ( $\pm 0.1$ )	0.7 ( $\pm 0.1$ )	~200	vertically
3-2	PCH506:(PCH50) <sub>2</sub> 6:(R)-D2 = 100:5:1	1.2	0.7 ( $\pm 0.1$ )	0.3 ( $\pm 0.1$ )	~130	horizontally
4	PCH506:(PCH50) <sub>2</sub> 6:(R)-D2 = 100:10:1	1.1	0.6 ( $\pm 0.1$ )	0.3 ( $\pm 0.1$ )	~250	vertically
5-1	PCH506:(PCH50) <sub>2</sub> 8:(R)-D2 = 100:3:0.5	2.4	1.2 ( $\pm 0.1$ )	0.6 ( $\pm 0.1$ )	~200	vertically
5-2	PCH506:(PCH50) <sub>2</sub> 8:(R)-D2 = 100:3:1	1.2	0.6 ( $\pm 0.1$ )	0.3 ( $\pm 0.1$ )	~150	horizontally
6-1	PCH506:(PCH50) <sub>2</sub> 8:(R)-D2 = 100:5:0.5	2.3	1.1 ( $\pm 0.1$ )	0.5 ( $\pm 0.1$ )	~150	vertically
6-2	PCH506:(PCH50) <sub>2</sub> 8:(R)-D2 = 100:5:1	1.1	0.6 ( $\pm 0.1$ )	0.3 ( $\pm 0.1$ )	~250	horizontally
7-1	PCH506:(PCH50) <sub>2</sub> 8:(R)-D2 = 100:10:0.5	2.4	1.2 ( $\pm 0.1$ )	0.6 ( $\pm 0.1$ )	~200	vertically
7-2	PCH506:(PCH50) <sub>2</sub> 8:(R)-D2 = 100:10:1	1.1	0.6 ( $\pm 0.1$ )	0.3 ( $\pm 0.1$ )	~250	horizontally
8	PCH506:(PCH50) <sub>2</sub> 6:(R)-D3 = 100:10:0.5	0.92	0.4 <sup>a</sup>	<sup>b</sup>	~400	vertically and bundle-free

<sup>a</sup> Interdistance between fibrils. <sup>b</sup> The helical pitch of system 8 is too small to form the bundle of fibrils.

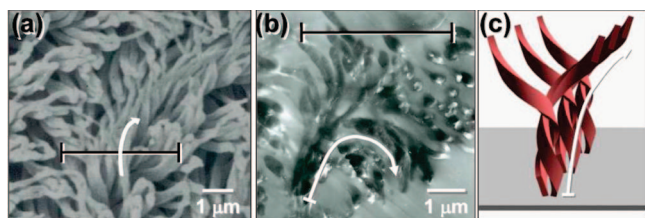


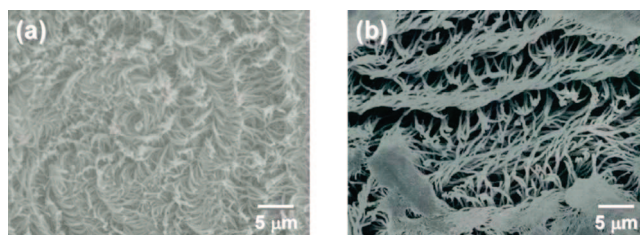
**Figure 2.** (a) SEM image of the surface of the vertically aligned H-PA. (b) TEM image of the cross section of the vertically aligned H-PA. The H-PA film was synthesized in the N\*-LC, System 1 [PCH506:(PCH50)<sub>2</sub>6:(R)-D1 = 100:3:2]. (c) Schematic representation of vertically aligned H-PA fibrils with left-handed screw direction.

range of temperature for the N\*-LC is favorable for the acetylene polymerization, because the exothermal heat inevitably evoking in the acetylene polymerization might raise the temperature inside a Schlenk flask and easily destroy the LC phase into an isotropic one (Table 3). Therefore, the high miscibility based on the liquid crystallinity of the chiral dopants, as well as the high HTPs, are important factors to prepare highly twisted N\*-LCs, irrespective of horizontally or vertically oriented reaction field.

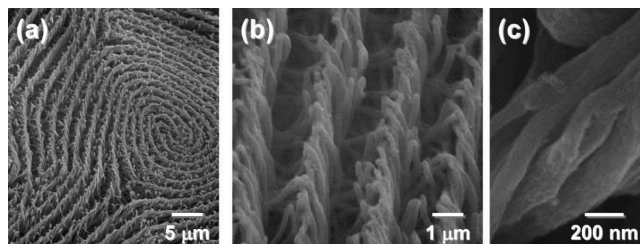
**4.3. Morphologies of H-PAs.** Figure 2 shows a SEM image of the H-PA synthesized in system 1 [PCH506 + (PCH50)<sub>2</sub>6 + (R)-D1]. The fibrils of the H-PA are vertically aligned and screwed with left-handed direction. The helical axis of the fibril bundle is perpendicular to the film surface. This is in contrast to the case of the horizontally aligned H-PA, where the helical axis is parallel to the film surface. As found in Figure 2, the fibrils of the H-PA grow perpendicular to the helical axis of the N\*-LC, in which the screw direction of the fibril bundle is opposite to that of the N\*-LC. This is in accordance with the mechanistic picture of Figure 1-f. The height of the vertically aligned fibril is estimated to be about 2  $\mu\text{m}$  on the basis of the TEM image of Figure 2-b.

Figure 3 shows the SEM images of the H-PA films synthesized in system 2 [PCH506 + (PCH50)<sub>2</sub>8 + (R)-D1]. The fibrils are vertically aligned but loosely screwed, forming a swirl of the fibril bundle (Figure 3a). When the concentration of the chiral dopant increases, the fibrils are highly screwed and grow rather parallel to the surface of the film (Figure 3b). It may be argued from comparison between Figures 2 and 3 that system 1 using (PCH50)<sub>2</sub>6 as the vertical orientation inducer is more favorable than system 2 using (PCH50)<sub>2</sub>8, so far as the formation of the vertically aligned and twisted fibril morphology is concerned.

Figures 4 and 5 show SEM images of the H-PA films synthesized in system 5-1 [PCH506 + (PCH50)<sub>2</sub>8 + (R)-D2].



**Figure 3.** SEM images of vertically aligned H-PAs synthesized in the N\*-LCs including D1 with various concentrations. Key: (a) system 2-1 [PCH506:(PCH50)<sub>2</sub>8:(R)-D1 = 100:3:1]; (b) system 2-2 [PCH506:(PCH50)<sub>2</sub>8:(R)-D1 = 100:3:2].



**Figure 4.** SEM images showing hierarchical spiral morphology of vertically aligned H-PAs synthesized in the N\*-LC including (R)-D2, system 5-1, [PCH506:(PCH50)<sub>2</sub>8:(R)-D2 = 100:3:0.5].

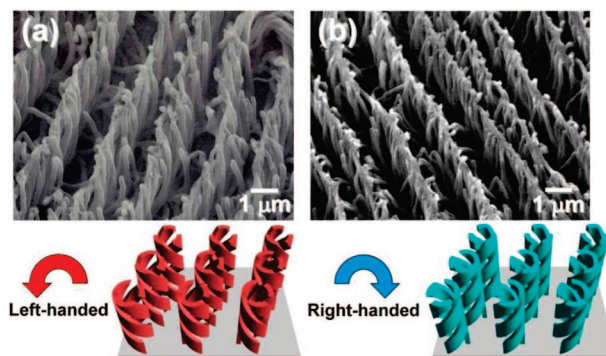


**Figure 5.** SEM images of the vertically aligned H-PAs synthesized in the N\*-LCs with opposite screwed structures. Key: (a) system 5-1 [PCH506:(PCH50)<sub>2</sub>8:(R)-D2 = 100:3:0.5]; (b) system 5-1 [PCH506:(PCH50)<sub>2</sub>8:(S)-D2 = 100:3:0.5].

The bundle of fibrils of the H-PA are vertically aligned and highly twisted in left-handed direction. The hierarchy in the helical structure is observed in the vertically aligned H-PA. Namely, the H-PA has a spiral morphology (Figure 4a), and each spiral is composed of bundles of vertically aligned fibrils with one-handed screwed direction (Figure 4b), and furthermore



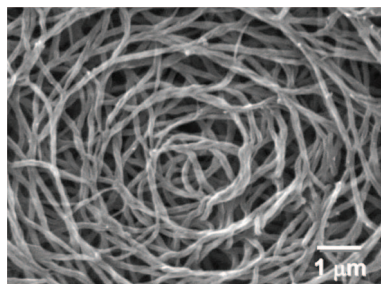


**Figure 6.** SEM image of H-PA synthesized in the N\*-LC, system 5-2 [PCH506:(PCH50)<sub>28</sub>:(R)-D2 = 100:3:1].

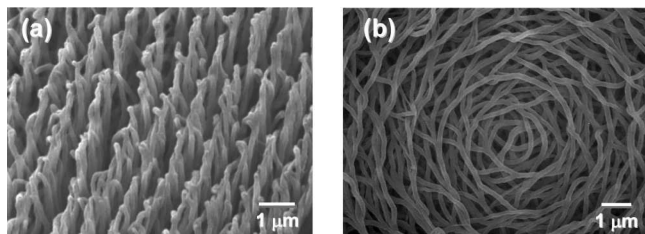


**Figure 7.** SEM images of H-PAs synthesized in the N\*-LCs including (R)-D2 with various concentrations. Key: (a) system 6-1 [PCH506:(PCH50)<sub>28</sub>:(R)-D2 = 100:5:0.5]; (b) system 6-2 [PCH506:(PCH50)<sub>28</sub>:(R)-D2 = 100:5:1].

the fibril itself is screwed with same direction of the bundles (Figure 4c). It is confirmed that the screw directions of the fibril and the bundle are opposite to the helical sense (right-handed screw direction) of the N\*-LC. As clearly seen in Figure 5, even the left- and right-handed screw directions of the vertically aligned fibrils are controllable by the chiral dopants of with (R)- and (S)-configurations, respectively.

**4.4. Balance between the Vertical Orientation Inducer and the Chiral Dopant.** The interdistances ( $d = 0.6\text{--}1.2\text{ }\mu\text{m}$ ) between the fibril bundles and the helical pitches ( $p = 1.1\text{--}2.4\text{ }\mu\text{m}$ ) of the fibrils of the H-PAs synthesized in systems 3 to 7 are shorter than those ( $d = 1.7\text{ }\mu\text{m}$ ,  $p = 3.6\text{ }\mu\text{m}$ ) in systems 1 or those ( $d = 1.5\text{--}2.8\text{ }\mu\text{m}$ ,  $p = 3.1\text{--}5.8\text{ }\mu\text{m}$ ) in system 2. This is because systems 3-7 have the chiral dopant of D2 whose HTP ( $\beta_M = 90\text{ }\mu\text{m}^{-1}$ ) is much larger than that of D1 ( $\beta_M = 18\text{ }\mu\text{m}^{-1}$ ) used in systems 1 or 2, and therefore, they serve for highly twisted N\*-LCs. However, it should be emphasized that the synthesis of the vertically aligned H-PA is not always guaranteed even if the chiral dopant with large HTP, such as D2, is used to prepare the N\*-LC. For instance, Figure 6 shows a SEM image of the H-PA synthesized in system 5-2 [PCH506:(PCH50)<sub>28</sub>:(R)-D2 = 100:3:1], where the helical pitch is  $1.2\text{ }\mu\text{m}$ . Although the H-PA has a spiral morphology consisting of helical fibrils, the fibrils are not vertically aligned, but horizontally aligned, i.e., lying on the surface. This may be due to the fact that the nature of the horizontal N\*-LC became too strong due to the relatively high concentration of the chiral dopant with large HTP, and that the concentration of the vertical orientation inducer [(PCH50)<sub>28</sub>] is too low to change the horizontal N\*-LC into the vertical one.

Figure 7 shows SEM images of the H-PAs synthesized in system 6-1 [PCH506:(PCH50)<sub>28</sub>:(R)-D2 = 100:5:0.5] and system 6-2 [PCH506:(PCH50)<sub>28</sub>:(R)-D2 = 100:5:1]. It is evident that the combination of the orientation inducer (PCH50)<sub>28</sub> and the chiral dopant D2 enabled us to control not only the vertical orientation but also horizontal one even in the N\*-LC and therefore those of the H-PAs. At the same time, it was found that the vertical and horizontal orientations in the present systems sensitively depend on the relative concentrations of the orientation inducer and the chiral dopant. For

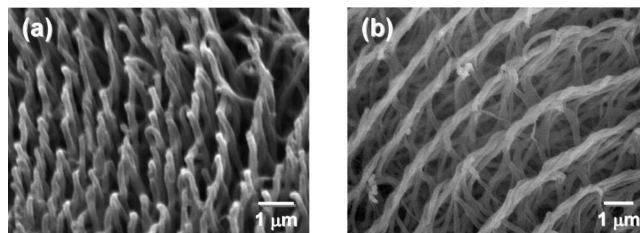


**Figure 8.** SEM images of H-PAs synthesized in the N\*-LCs including D2 with vertical orientation inducer. Key: (a) system 4 [PCH506:(PCH50)<sub>26</sub>:(R)-D2 = 100:10:1]; (b) system 7-2 [PCH506:(PCH50)<sub>28</sub>:(R)-D2 = 100:10:1].

instance, in a concentration where the nature of the orientation inducer (PCH50)<sub>28</sub> becomes stronger than that of the chiral dopant D2, the LC shows a vertical orientation of helically twisted structure; However, in another concentration where the nature of the former becomes weaker than that of the latter, the LC shows a horizontal orientation of helically twisted structure. The chiral dopants (D1 and D2) have a tendency to align the parent LC horizontally as well as a tendency to twist it in one-handed direction. Therefore a certain amount of the vertical orientation inducer, (PCH50)<sub>26</sub> or (PCH50)<sub>28</sub>, is required to prepare the vertically aligned and helically twisted N\*-LC.

**4.5. Horizontal and Vertical Alignments.** Figure 8 shows the SEM images of the H-PA films synthesized in system 4 [PCH506:(PCH50)<sub>26</sub>:(R)-D2 = 100:10:1] and system 7-2 [PCH506:(PCH50)<sub>28</sub>:(R)-D2 = 100:10:1]. Although both systems have the same components and concentrations except the vertical orientation inducer, system 4 and system 7-2 gave the vertically aligned and horizontally aligned H-PAs, respectively. As far as the synthesis of vertically aligned H-PA is concerned, the former (system 4) is more preferable than the latter (system 7-2).

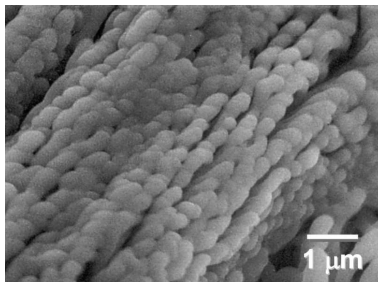
In the vertical but nonhelically twisted orientation of N-LC, (PCH50)<sub>28</sub> shows a stronger ability to align the parent LC molecules [PCH506] than (PCH50)<sub>26</sub>. On the contrary, (PCH50)<sub>28</sub> shows a less ability as a vertical orientation inducer than (PCH50)<sub>26</sub> in the case of the vertical and helically twisted orientation, as clarified here. This indicates that the ability of the vertical orientation inducer depends on the matching in molecular structure between the chiral dopant and the parent LC in nonhelical or helical LC environment.

Table 4 summarizes the helical pitches of N\*-LCs (systems 1 to 7) and the structural parameters, such as the interdistances between the fibril bundles, the diameters of the fibril bundle and those of the fibrils, as well as the directions of fibril alignment of the H-PAs. It is confirmed through the table that the interdistance ( $d$ ) between the fibril bundles almost equals to a half of the helical pitches ( $p$ ),  $d = p/2$ , and that this relationship holds irrespective of the direction of the fibril alignment.

Besides, it is worthy noting that although the fibril bundles decrease in diameter with decreasing in helical pitch (i.e., with increasing in helical twist) of the N\*-LC, the fibril remains unchanged, keeping the diameter in the range of 150 to 250 nm. This suggests that when acetylene polymerization is carried out in the highly twisted N\*-LC, the resultant H-PA may not form the bundle of the fibrils, but give bundle-free fibrils, as currently found in the ordinary (horizontally aligned) H-PA.<sup>6c</sup> This motivates us to use the chiral dopant with much larger HTP, as will be discussed below.

#### 4.6. Vertically Aligned H-PAs with Bundle-Free Fibrils.

Figure 9 shows a SEM image of the H-PA film synthesized in system 8 [PCH506:(PCH50)<sub>26</sub>:(S)-D3 = 100:5:0.5]. System 8 is a highly twisted N\*-LC having a helical pitch of 920 nm,



**Figure 9.** SEM image of H-PA synthesized in the N\*-LC including (S)-D3, system 8 [PCH506:(PCH50)<sub>2</sub>6:(S)-D3 = 100:5:0.5].

because it includes the *tetra*-substituted binaphthyl derivative (D3), as a chiral dopant, whose HTP ( $240 \mu\text{m}^{-1}$ ) is ca. 2.7 times larger than that ( $90 \mu\text{m}^{-1}$ ) of D2, as mentioned before. It is seen in Figure 9 that the H-PA has right-handed and vertically aligned fibrils, but it has no bundle of the fibrils. This is in quite contrast to the morphology of other H-PAs synthesized in systems 1 to 7. Such a difference in morphology may be explained as follows.

In the weakly twisted N\*-LCs (systems 1 to 7) whose helical pitches are larger than  $1 \mu\text{m}$ , the fibrils of the resultant H-PA are gathered, owing to van der Waals interactions, to form the bundle of fibrils. Therein, the diameters of the fibril and the bundle are 150–250 nm and about  $1 \mu\text{m}$ , respectively. On the other hand, in the strongly twisted N\*-LC (system 8) whose helical pitch is smaller than  $1 \mu\text{m}$ , the resultant H-PA has highly screwed fibrils but not the bundle of fibrils. This is because, the helical pitch of 920 nm of system 8 is too small to form the bundle of fibrils. The morphology free from the bundle of fibrils might be useful to evaluate electromagnetic properties of the vertically aligned and screwed fibril.

## 5. Conclusion

Macroscopically aligned H-PAs are synthesized in the orientation-controlled N\*-LCs. The N\*-LCs are prepared by adding the vertical orientation inducer [(PCH50)<sub>2</sub>6 or (PCH50)<sub>2</sub>8] and the chiral dopant (the binaphthyl derivatives such as D1, D2, or D3) into the parent N-LC [PCH506]. It is found that the horizontal or vertical orientation of the N\*-LC crucially depends on (i) the relative concentrations of the vertical orientation inducer and the chiral dopant, (ii) the miscibility of the vertical orientation inducer to the parent N-LC, and (iii) the helical twisting power of the chiral dopant. In other words, the balance in effectiveness of the roles between the vertical orientation inducer and the chiral dopant dominates the macroscopic orientation of the N\*-LC and hence the morphological alignment resultant of the H-PA. The present orientation-controllable N\*-LCs are useful for the synthesis of macroscopically aligned conjugated polymers, allowing the morphological control without any external force or oriented substrate.

**Acknowledgment.** The authors are grateful to a colleague of laboratory, Mr. M. Goh, for his generous supply of the chiral dopant

of D3. This work was supported by a Grant-in-Aid for Science Research (S) (No. 20225007) and that in a Priority Area “Super-Hierarchical Structures” (Grant No. 446) from the Ministry of Education, Culture, Sports, Science and Technology, Japan.

## References and Notes

- (1) (a) Chien, J. C. W. *Polyacetylene: Chemistry, Physics and Material Science*; Academic Press: Orlando, FL, 1984; Chapter 2. (b) Naarmann, H.; Theophilou, N. *Synth. Met.* **1987**, *22*, 1. (c) Araya, K.; Mukoh, A.; Narahara, T.; Shirakawa, H. *Chem. Lett.* **1984**, 1141. (d) Akagi, K.; Shirakawa, H.; Araya, K.; Mukoh, A.; Narahara, T. *Polym. J.* **1987**, *19*, 185. (e) Akagi, K.; Katayama, S.; Shirakawa, H.; Araya, K.; Mukoh, A.; Narahara, T. *Synth. Met.* **1987**, *17*, 241. (f) Akagi, K.; Suezaki, M.; Shirakawa, H.; Kyotani, H.; Shimomura, M.; Tanabe, Y. *Synth. Met.* **1989**, *28*, D1.
- (2) (a) Montaner, A.; Rolland, M.; Sauvajol, J. L.; Galtier, M.; Almairac, R.; Ribet, J. L. *Polymer* **1988**, *29*, 1101. (b) Coustel, N.; Foxonet, N.; Ribet, J. L.; Bernier, P.; Fischer, J. E. *Macromolecules* **1991**, *24*, 5867.
- (3) (a) Akagi, K.; Piao, G.; Kaneko, S.; Sakamaki, K.; Shirakawa, H.; Kyotani, M. *Science* **1998**, *282*, 1683. (b) Akagi, K.; Higuchi, I.; Piao, G.; Shirakawa, H.; Kyotani, M. *Mol. Cryst. Liq. Cryst.* **1999**, *332*, 463. (c) Piao, G.; Akagi, K.; Shirakawa, H. *Synth. Met.* **1999**, *101*, 92. (d) Akagi, K.; Piao, G.; Kaneko, S.; Higuchi, I.; Shirakawa, H.; Kyotani, M. *Synth. Met.* **1999**, *102*, 1406. (e) Akagi, K.; Higuchi, I.; Piao, G.; Shirakawa, H.; Kyotani, M. *Mol. Cryst. Liq. Cryst.* **1999**, *332*, 2973. (g) Akagi, K.; Guo, S.; Mori, T.; Goh, M.; Piao, G.; Kyotani, M. *J. Am. Chem. Soc.* **2005**, *127*, 14647. (h) Akagi, K. In *Handbook of Conducting Polymers, Conjugated Polymers*, 3rd ed.; Skotheim, T. A., Reynolds, J. R., Eds.; CRC Press: New York, 2007; pp 3–14. (i) Akagi, K. *Polym. Int.* **2007**, *56*, 1192.
- (4) (a) Kang, S. W.; Jin, S. H.; Chien, L. C.; Sprunt, S. *Adv. Funct. Mater.* **2004**, *14*, 329. (b) Goto, H.; Akagi, K. *Angew. Chem., Int. Ed.* **2005**, *44*, 4322. (c) Goto, H.; Akagi, K. *Macromolecules* **2005**, *38*, 1091. (d) Goto, H.; Jeong, Y. S.; Akagi, K. *Macromol. Rapid Commun.* **2005**, *26*, 164. (e) Goto, H.; Akagi, K. *Chem. Mater.* **2006**, *18*, 255. (f) Kyotani, M.; Matsushita, S.; Nagai, T.; Matsui, Y.; Shimomura, M.; Kaito, A.; Akagi, K. *J. Am. Chem. Soc.* **2008**, *130*, 10880.
- (5) (a) Heppke, G.; Löttsch, D.; Oestreich, F. Z.; Naturforsch., A. *J. Phys. Sci.* **1986**, *41*, 1214. (b) Rokunohe, A.; Yoshizawa, J. *Mater. Chem.* **2005**, *15*, 275.
- (6) (a) Gottarelli, G.; Mariani, P.; Spada, G. P.; Samori, B.; Forni, A.; Solladie, G.; Hibert, M. *Tetrahedron* **1983**, *39*, 1337. (b) Goh, M.; Kyotani, M.; Akagi, K. *J. Am. Chem. Soc.* **2007**, *129*, 8519. (c) Goh, M.; Matsushita, T.; Kyotani, M.; Akagi, K. *Macromolecules* **2007**, *40*, 4762. (d) Mori, T.; Kyotani, M.; Akagi, K. *Macromolecules* **2008**, *41*, 607.
- (7) (a) Piao, G.; Otake, T.; Sato, T.; Akagi, K.; Kyotani, M. *Mol. Cryst. Liq. Cryst.* **2001**, *365*, 117. (b) Shirakawa, H.; Otake, T.; Piao, G.; Akagi, K.; Kyotani, M. *Synth. Met.* **2001**, *117*, 1. (c) Mori, T.; Sato, T.; Kyotani, M.; Akagi, K. *Synth. Met.* **2003**, *135*, 83.
- (8) Kanazawa, K.; Higuchi, I.; Akagi, K. *Mol. Cryst. Liq. Cryst.* **2001**, *364*, 825.
- (9) (a) Grandjean, F. C. R. *Acad. Sci.* **1921**, 172. (b) Cano, R. *Bull. Soc. Fr. Mineral.* **1968**, *91*, 20. (c) Heppke, G.; Oestreich, F. *Mol. Cryst. Liq. Cryst. Lett.* **1978**, *41*, 245. (d) Gottarelli, G.; Samori, B.; Stremmenos, C.; Torre, G. *Tetrahedron* **1981**, *37*, 395.
- (10) (a) Friedel, G. *Ann. Phys. (Paris)* **1922**, *18*, 273. (b) Yoshida, J.; Sato, H.; Yamagishi, A.; Hoshino, N. *J. Am. Chem. Soc.* **2005**, *127*, 8453.
- (11) Kuball, H. G.; Höfer, T. In *Chirality in Liquid Crystals*; Kitzrow, H. S., Bahr, C., Eds.; Springer Press: New York, 2000; Vol. 1, Chapter 3, p 67.
- (12) (a) Heppke, G.; Oestreich, F. *Mol. Cryst. Liq. Cryst. Lett.* **1978**, *41*, 245. (b) Uchida, T.; Inukai, T. In *Liquid Crystal-Fundamentals*; Okano, K., Kobayashi, S., Eds.; Baifukan: Tokyo, 1985; pp 205–231.

MA9000034